Seasonal Erosion and Restoration of Mars' Northern Polar Dunes

C. J. Hansen, *et al.*

Science **331**, 575 (2011);
DOI: 10.1126/science.1197636

hanced aromatic sequon as a portable stabilizing module for research and therapeutic applications.

References and Notes

1. R. Kornfeld, S. Kornfeld, *Annu. Rev. Biochem.* **54**, 631 (1985).
2. M. Molinari, *Nat. Chem. Biol.* **3**, 313 (2007).
3. A. Helenius, M. Aebi, *Science* **291**, 2364 (2001).
4. R. Glozman *et al.*, *J. Cell Biol.* **184**, 847 (2009).
5. M. R. Wormald *et al.*, *Eur. J. Biochem.* **198**, 131 (1991).
6. A. H. Andreotti, D. Kahne, *J. Am. Chem. Soc.* **115**, 3352 (1993).
7. B. Imperiali, K. W. Rickert, *Proc. Natl. Acad. Sci. U.S.A.* **92**, 97 (1995).
8. C. Wang, M. Eufemi, C. Turano, A. Giartosio, *Biochemistry* **35**, 7299 (1996).
9. H. Yamaguchi, M. Uchida, *J. Biochem.* **120**, 474 (1996).
10. G. Kern, N. Schülke, F. X. Schmid, R. Jaenicke, *Protein Sci.* **1**, 120 (1992).
11. S. R. Hanson *et al.*, *Proc. Natl. Acad. Sci. U.S.A.* **106**, 3131 (2009).
12. G. Walsh, R. Jefferis, *Nat. Biotechnol.* **24**, 1241 (2006).
13. M. M. Chen *et al.*, *Proc. Natl. Acad. Sci. U.S.A.* **107**, 22528 (2010).
14. S. Elliott, D. Chang, E. Delorme, T. Eris, T. Lorenzini, *J. Biol. Chem.* **279**, 16854 (2004).
15. J. L. Price *et al.*, *J. Am. Chem. Soc.* **132**, 15359 (2010).
16. D. F. Wyss *et al.*, *Science* **269**, 1273 (1995).
17. B. L. Sibanda, T. L. Blundell, J. M. Thornton, *J. Mol. Biol.* **206**, 759 (1989).
18. Materials and methods are available as supporting material on *Science* Online.
19. E. Y. Jones, S. J. Davis, A. F. Williams, K. Harlos, D. I. Stuart, *Nature* **360**, 232 (1992).
20. A. Horovitz, A. R. Fersht, *J. Mol. Biol.* **224**, 733 (1992).
21. C. D. Geierhaas, E. Paci, M. Vendruscolo, J. Clarke, *J. Mol. Biol.* **343**, 1111 (2004).
22. A. Pastore, V. Saudek, G. Ramponi, R. J. P. Williams, *J. Mol. Biol.* **224**, 427 (1992).
23. R. C. Y. Yeung, S. Y. Lam, K. B. Wong, *Acta Crystallogr. Sect. F* **62**, 80 (2006).
24. A.-J. Petrescu, A.-L. Milac, S. M. Petrescu, R. A. Dwek, M. R. Wormald, *Glycobiology* **14**, 103 (2004).
25. Z. R. Laughrey, S. E. Kiehna, A. J. Riemen, M. L. Waters, *J. Am. Chem. Soc.* **130**, 14625 (2008).
26. R. Ranganathan, K. P. Lu, T. Hunter, J. P. Noel, *Cell* **89**, 875 (1997).
27. B. Imperiali, K. L. Shannon, M. Unno, K. W. Rickert, *J. Am. Chem. Soc.* **114**, 7944 (1992).
28. D. F. Zielinska, F. Gnad, J. R. Wiśniewski, M. Mann, *Cell* **141**, 897 (2010).
29. R. Apweiler, H. Hermjakob, N. Sharon, *Biochim. Biophys. Acta* **1473**, 4 (1999).
30. Single-letter abbreviations for the amino acid residues are as follows: A, Ala; E, Glu; F, Phe; G, Gly; H, His; I, Ile; K, Lys; L, Leu; M, Met; N, Asn; R, Arg; S, Ser; and T, Thr.

31. We thank R. A. Dwek, I. A. Wilson, J. C. Paulson, S. Deechongkit, and D. L. Powers for presubmission reviews and for helpful prepublication discussions. This work was supported in part by the Skaggs Institute for Chemical Biology, the Lita Annenberg Hazen Foundation, and by NIH grant GM051105 to J.W.K. and E.T.P. J.L.P. was supported in part by NIH postdoctoral fellowship F32 GM086039. A.D. and M.G. were supported by NSF grant MCB 1019958. S.R.H. and C.-H.W. were supported by NIH grant AI072155. The Scripps Research Institute has filed a provisional patent application covering the results described in this paper.

Supporting Online Material

www.sciencemag.org/cgi/content/full/331/6017/571/DC1
Materials and Methods
SOM Text
Figs. S1 to S18
Tables S1 to S3
References

29 September 2010; accepted 5 January 2011
10.1126/science.1198461

Seasonal Erosion and Restoration of Mars' Northern Polar Dunes

C. J. Hansen,[1]* M. Bourke,[1,2] N. T. Bridges,[3] S. Byrne,[4] C. Colon,[5] S. Diniega,[6] C. Dundas,[4] K. Herkenhoff,[7] A. McEwen,[4] M. Mellon,[8] G. Portyankina,[9] N. Thomas[9]

Despite radically different environmental conditions, terrestrial and martian dunes bear a strong resemblance, indicating that the basic processes of saltation and grainfall (sand avalanching down the dune slipface) operate on both worlds. Here, we show that martian dunes are subject to an additional modification process not found on Earth: springtime sublimation of Mars' CO_2 seasonal polar caps. Numerous dunes in Mars' north polar region have experienced morphological changes within a Mars year, detected in images acquired by the High-Resolution Imaging Science Experiment on the Mars Reconnaissance Orbiter. Dunes show new alcoves, gullies, and dune apron extension. This is followed by remobilization of the fresh deposits by the wind, forming ripples and erasing gullies. The widespread nature of these rapid changes, and the pristine appearance of most dunes in the area, implicates active sand transport in the vast polar erg in Mars' current climate.

Mars has a vast region of dark sand dunes at high northern latitudes (*1*), initially identified in Mariner 9 images (*2*, *3*). Viking images of changing dune profiles, sediment streamers from barchan horns, and pristine dune morphology suggested that the dunes were active (*4*, *5*), but only limited dune change such as the erosion of four small dome dunes were apparent in more recent mission images (*6*, *7*). Most data suggested that the north polar dunes are currently stable—possibly indurated or crusted (*6*, *8*). Recent High-Resolution Imaging Science Experiment (HiRISE) images show, however, that substantial sediment transport does occur today on martian north polar dune slipfaces, via grainflow triggered by seasonal CO_2 sublimation.

Every year, Mars' polar regions are covered by seasonal caps of CO_2 frost (*9*). Northern springtime phenomena associated with sublimation of this seasonal layer were first imaged by the Mars Orbiter Camera (MOC) in 1999 (*10*). In recent high-resolution (~1 m) HiRISE images, spring sublimation activity appears as fans, bright-dark rings, and dark streaks initiated at dune brinks (*11*). HiRISE has imaged seasonal activity for two Mars years: MY29 and MY30 (*12*); its high signal-to-noise ratio (SNR) facilitates imaging at low light levels in early spring and enables detection of very subtle changes on the dark dunes (*13*).

Mass wasting was observed on northern dunes in MY29 images, and grainflow due to sublimation of CO_2 was identified as a potential cause of the dark streaks (*11*). Other possibilities included

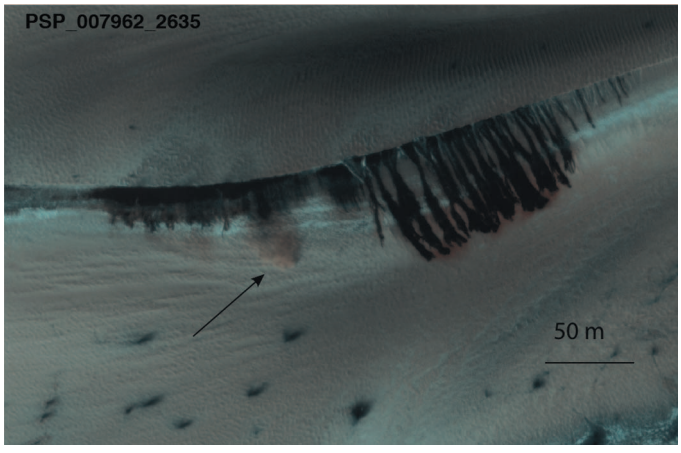

Fig. 1. Slope streaks and a small cloud of dust (arrow) kicked up by sand and ice cascading down the dune slope are captured in this subimage acquired at 83.5°N, 118.6°E. Imaged at $L_s = 55.7$ (*35*), dunes are still covered by seasonal ice. This particular dune is ~40 m high. North is up; light is from the lower left. The dark slope streaks visible in the image are postulated to be sand that has been released from the brink of the dune to slide down and cover seasonal ice.

[1]Planetary Science Institute, Tucson, AZ 85719, USA. [2]School of Geography and the Environment, University of Oxford, Oxford OX1 3QY, UK. [3]Applied Physics Lab, John Hopkins University, Laurel, MD 20723, USA. [4]Lunar and Planetary Laboratory, University of Arizona, Tucson, AZ 85721, USA. [5]Department of Earth and Environmental Science, Rutgers University, Newark, NJ 07102, USA. [6]Jet Propulsion Laboratory, California Institute of Technology, Pasadena, CA 91109, USA. [7]U.S. Geological Survey, Flagstaff, AZ 86001, USA. [8]Laboratory for Atmospheric and Space Physics, University of Colorado, Boulder, CO 80309, USA. [9]Space Research and Planetology Division, University of Bern, CH-0132 Bern, Switzerland.

*To whom correspondence should be addressed. E-mail: cjhansen@psi.edu

differential sublimation of CO_2 ice due to ripple morphology, subtle differences in lighting, or a difference in the translucency of the seasonal ice layer. Liquid salt brine flow has also been proposed (*14*–*16*) as the explanation for dark streaks but requires temperatures of >200 K. Such temperatures imply a frost-free surface, which is inconsistent with early spring observations of the dark streaks.

On the basis of observations of changes in dune morphology detected from MY29 to MY30, we assert that these streaks are activated seasonally and are caused by sand and ice cascading down the slipfaces of the dunes (*17*), as captured in Fig. 1. The correlation of changes—including new headcuts, short gullies, and apron extensions—with seasonal activity are shown in Fig. 2. In the full 6.4-by 19.2-km image of the dune field, ~20% of the dunes show substantial modification (measurable changes), whereas another ~20% show minor modification (detectable but too small to quantify).

The time series that the seasonal activity follows is illustrated in Fig. 3. The dune in Fig. 3A has a steep upper lee slope, with small grainflows and a lower-angle dune apron covered by wind ripples. One Mars year later (Fig. 3B), two large grainflows with well-developed head scarps have cut back into the dune brink. Their associated depositional lobes have buried wind ripples and deposited sediment beyond the dune footslope. Figure 3, C to E, shows the development of dark sediment streaks on the dune as sand is mobilized. We postulate that this sediment transport is driven by the destabilizing gas flow of CO_2 sublimation.

We have observed similar changes on dunes in >40% of the locations in the north polar region imaged more than once by HiRISE, suggesting that many of the dunes in the north polar sand seas are being eroded in the spring. At high latitudes in the southern hemisphere, CO_2-triggered flow has been proposed as an agent of dune modification—for example, in Matara crater (*18*). Seasonally constrained dune modification and gully development is also reported for dune gully (*19*, *20*) and slope gully (*21*) activity in the southern hemisphere. Examination of 25 image pairs on nonpolar dunes (60°N to 40°S latitude) shows no change in dune morphology, reinforcing the apparent requirement for CO_2 frost as the agent for initiating sediment transport.

When the sun rises in the spring, it first illuminates the highest and steepest part of the dune, the brink. As the CO_2 layer at the brink starts to sublimate, it thins and weakens. The brink also experiences the highest extensional stress from gravitational downslope loads on the CO_2 ice layer, leading to rupture of the ice layer via cracks, such as those in Fig. 3C. A model developed for the southern hemisphere to explain a variety of seasonal phenomena postulates that insolation through translucent ice combined with subsurface heat conduction leads to basal sublimation of the seasonal CO_2 ice layer (*22*–*25*). The gas, trapped under the ice, will escape through cracks, entraining surface material (*26*–*29*). We propose that a similar process could be active in the northern hemisphere dunes and that it is at the brink of the dune that a rupture is most likely to occur, allowing gas to escape. A numerical model predicts that pressurized gas flow from basal sublimation of

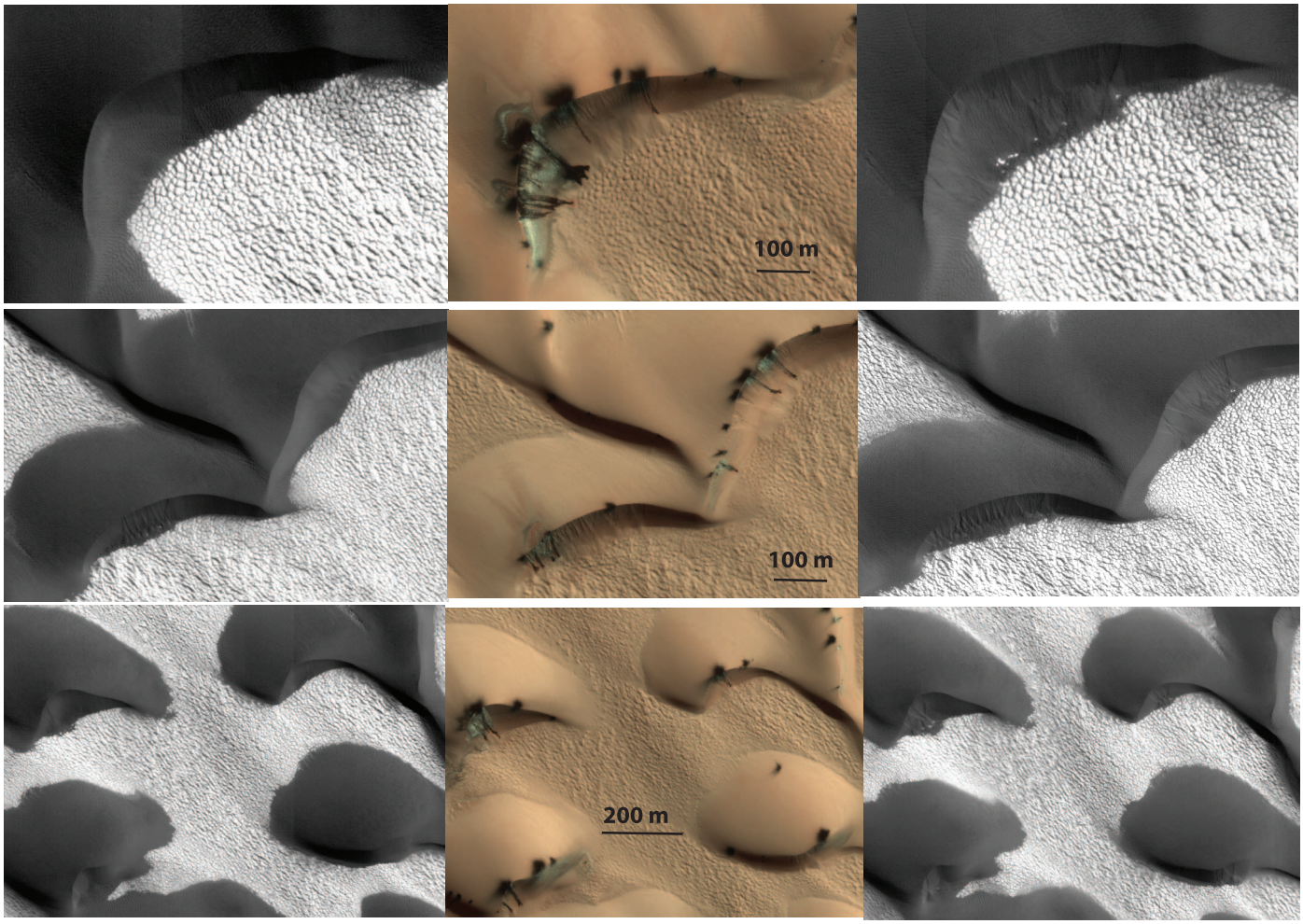

Fig. 2. A time-series of subimages, from left to right, at three sites in a field of transverse dunes at 84.7°N, 0.7°E shows that extensive erosion has taken place in one Mars year. The center false-color strip are subimages from ESP_016893_2650 taken on 4 March 2010, L_s = 59.6 when the region was still covered with seasonal CO_2 ice. The black-and-white ice-free subimages compare PSP_009324_2650 (left subimage in each row), acquired on 23 July 2008, L_s = 102.4 in MY29, with ESP_017974_2650 (right subimage in each row) acquired on 28 May 2010, L_s = 96.6 in MY30, the second year of HiRISE monitoring. North is down; light is from the upper right. These subtle changes on dark dunes would have been very difficult to detect in past images without the SNR of HiRISE.

CO_2 may reach 10 m/s under the ice slab, which is enough to mobilize loose grains of sand [supporting online material (SOM) text]. Tiny channels just barely detectable on the stoss side of the dune may be gas conduits to the dune brink (Fig. 2, blue arrow). In addition to sublimation processes, frozen CO_2 could abet mass movement through overloading on the dune face to cause avalanching; chunks of ice are seen at the bottom of the slipface in Fig. 2. Sublimating CO_2 gas permeating the uppermost level of the sand may reduce its cohesion.

We analyzed five of the dunes shown in Fig. 2 in order to quantify advancement of the dune slipface foot. The offset in contact between the lee edge and the underlying patterned ground was measured in two co-registered ice-free images (Fig. 4). Differences ranged from 2.2 to 4.7 m, with an average of 3.3 m/year. In three of the five dunes, there were changes in the stoss position. Unlike the lee foot slope, the stoss margin both advanced and retreated in two of the dunes, with the third showing just advancement. Average advance rates ranged from 0.7 to 1.4 m/year, with retreat ranging from 0.4 to 2 m/year. For the three dunes on which we measured stoss and lee changes, 7 to 14 ripples on the edges of the dunes advanced between 0.7 to 1.6 m, which is comparable with rates of dune ripple migration in Nili Patera (*30*). These results indicate that both wind and CO_2 sublimation play a role in transporting sand on the dunes. The expansion of the stoss slope in some places suggests that winds are not unidirectional.

Mars' northern hemisphere dunes may contain large amounts of water ice internally, but the upper 6 to 25 cm of sand are expected to be desiccated if the water ice is in vapor-diffusive equilibrium with

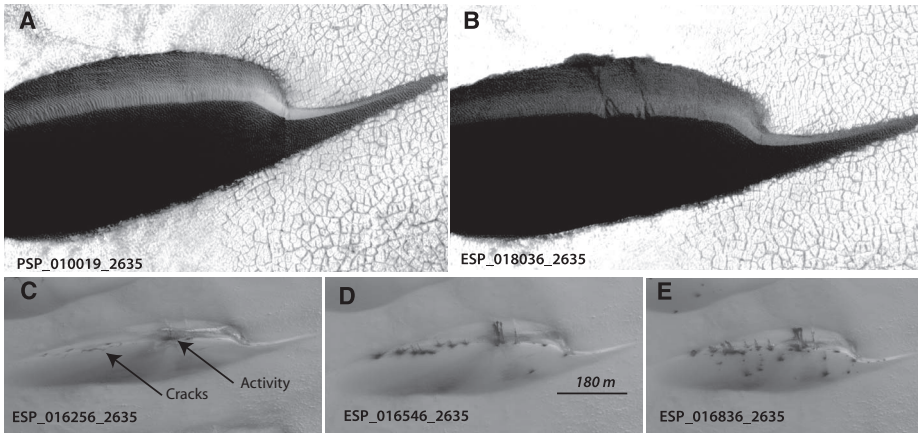

Fig. 3. This series acquired at 83.5N, 118.5 E illustrates sublimation activity and the redistribution of sand on the slipface. North is down in all images; sunlight is coming from the upper right. Slipfaces are oriented to the south in this dune field. (**A**) This subimage taken 15 September 2008 at L_s = 127.4 in the first year of HiRISE monitoring shows the ice-free dune. (**B**) A subimage acquired in the second year of HiRISE monitoring, 1 June 2010 at L_s = 98.7 after seasonal ice has sublimed, shows two new grainflows on the dune. (**C**) 14 January 2010 frosted subimage at L_s = 37.6 shows that sand has moved part of the way down the dune and appears to be blocked by a thin ledge of bright ice. Visible are cracks in the ice along the brink of the dune on the left side. Dark material on the stoss side of the dune may be patches of thin ice or dune material blown backward by the sublimation gas flow. (**D**) 5 February 2010, subimage at L_s = 47.7 shows that sand has moved further down the slipface. Other smaller slides are initiated at the crack in the ice along the brink of the dune. (**E**) 28 February 2010, L_s = 57.7. Sand has now started to accumulate at the foot of the slope, and other streaks are lengthening.

Fig. 4. The dune margin in MY29 image PSP_008968_2650 at 84.7°N, 0.7°E is compared with MY30 ESP_017895_2650.

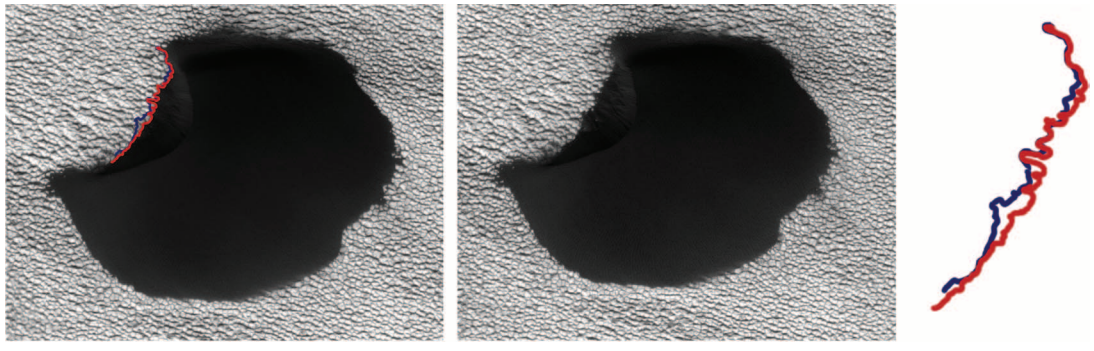

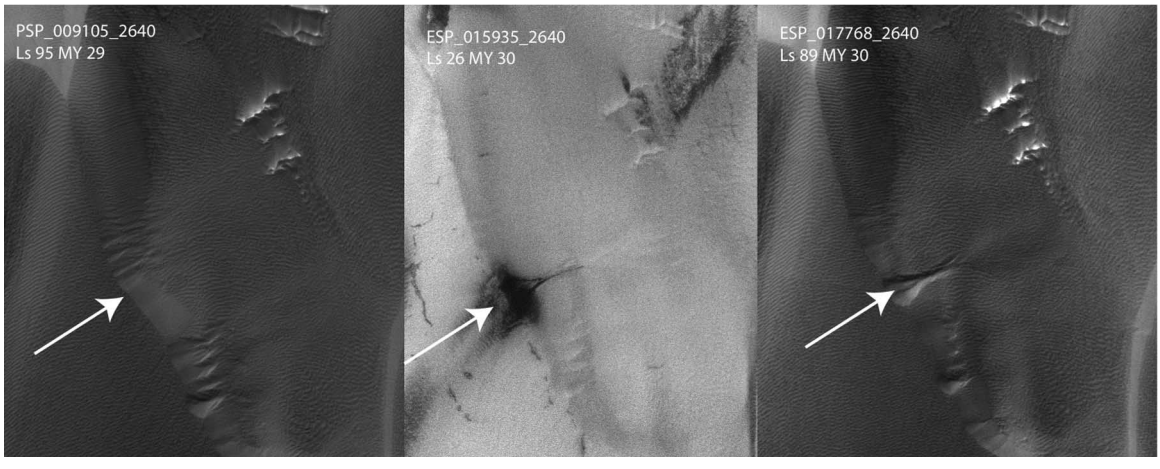

Fig. 5. The white arrows point to a location on the brink of this dune at 84°N, 233°E that had no alcove in the first year of HiRISE operation (MY29) and experienced sublimation activity (middle), which resulted in the new alcove and fan (with total length of 120 m) in MY30. The layer of new material forming the apron is very thin; the original ripples have not been completely buried. Degradation of gullies is also occurring, as adjacent alcoves are being filled in, and ripples are already forming in the alcoves.

the atmosphere (*31*, *32*). The style of activity imaged requires that the observed slipfaces are not strongly ice-cemented within the erosion depths. Some of the new grainflow alcoves have widths of tens of meters and have recessed in excess of 10 m into the brink. This implies transport of hundreds of cubic meters of sand (fig. S1). Even intermediate-sized gullies such as that in Fig. 5 require movement of tens of cubic meters of sediment.

The reworking of older gully alcoves by aeolian ripples is shown in Fig. 5. The recovery rate of the slipface and the existence of smooth slopes (no grainflows) suggests that grainflow formation and remobilization of sediment by wind may be approximately in equilibrium on a multiyear time scale, although relative rates could vary annually. The seasonal-scale frequency of these two processes demonstrates active sediment transport on polar dunes in the current martian climate. Whether they indicate migration of martian dune forms or simply represent the crestline maintenance of nonmobile dunes can only be determined with future multiyear observations.

In locations where wind energy is insufficient to reconstitute grainflow scars, modification of dune form should ensue. With an estimated sediment transport that delivers tens to hundreds of cubic meters of sand in one Mars year to the dune foot slopes, the initial modification of dune form would be rapid. Resulting dune morphologies would have rounded crests, no brinks, and long, low-angle footslopes. This mechanism may explain some of the unusual dune forms reported on Mars (*33*). However, because the majority of Mars' north polar dunes do not assume this morphology, we suggest that maintenance of the dune form is an active process under the current martian climate.

References and Notes

1. M. R. Balme, D. Berman, M. Bourke, J. Zimbelman, *Geomorphology* **101**, 703 (2008).
2. J. F. McCauley *et al.*, *Icarus* **17**, 289 (1972).
3. J. A. Cutts, R. S. U. Smith, *J. Geophys. Res.* **78**, 4139 (1973).
4. H. Tsoar, R. Greeley, A. R. Peterfreund, *J. Geophys. Res.* **84** (B14), 8167 (1979).
5. A. W. Ward, K. B. Doyle, *Icarus* **55**, 420 (1983).
6. M. C. Bourke, K. Edgett, B. Cantor, *Geomorphology* **94**, 247 (2008).
7. M. C. Bourke *et al.*, *Proc. Lunar Planet. Sci. Conf.* **40**, 1748 (2009).
8. V. Schatz, H. Tsoar, K. S. Edgett, E. J. R. Parteli, H. J. Herrmann, *J. Geophys. Res.* **111** (E4), E002514 (2006).
9. In this paper, we use "frost" and "ice" somewhat interchangeably. Martian snow has been shown to increase in density as the winter season progresses (*34*), so usage of this terminology transitions from one to the other. Readers are encouraged to understand the use of either term to be synonymous with "seasonally condensed volatile."
10. M. Malin, K. Edgett, *J. Geophys. Res.* **106** (E10), 23429 (2001).
11. C. J. Hansen *et al.*, *Bull. Am. Astron. Soc.* **40**, 409 (2008).
12. The numbering of Mars years was defined to facilitate comparison of data sets across decades and multiple Mars missions. Year 1 started 11 April 1955.
13. A. McEwen *et al.*, *J. Geophys. Res.* **112** (E5), E002605 (2007).
14. A. Kereszturi *et al.*, *Icarus* **201**, 492 (2009).
15. A. Kereszturi *et al.*, *Icarus* **207**, 149 (2010).
16. D. Möhlmann, A. Kereszturi, *Icarus* **207**, 654 (2010).
17. C. Hansen *et al.*, *Proc. Lunar Planet. Sci. Conf.* **41**, 1533 (2010).
18. M. C. Malin, K. Edgett, NASA/JPL Planetary Photojournal, http://photojournal.jpl.nasa.gov/, catalog no. PIA04290 (2005).
19. S. Diniega, S. Byrne, N. T. Bridges, C. M. Dundas, A. S. McEwen, *Geology* **38**, 1047 (2010).
20. E. Gardin, P. Allemand, C. Quantin, P. Thollot, *J. Geophys. Res.* **115** (E6), E06016 (2010).
21. C. M. Dundas, A. S. McEwen, S. Diniega, S. Byrne, S. Martinez-Alonso, *Geophys. Res. Lett.* **37**, L07202 (2009).
22. H. H. Kieffer, Lunar and Planetary Institute contribution 1057 (2000).
23. S. Piqueux, P. R. Christensen, *J. Geophys. Res.* **113** (E6), E06005 (2003).
24. O. Aharonson, 35th Lunar and Planetary Science Conference, 15 to 19 March 2004, League City, TX, abstr. 1918 (2004).
25. H. Kieffer, *J. Geophys. Res.* **112** (E8), E08005 (2007).
26. S. Piqueux, P. R. Christensen, *J. Geophys. Res.* **113** (E6), E06005 (2008).
27. C. J. Hansen *et al.*, *Icarus* **205**, 283 (2010).
28. N. Thomas, C. J. Hansen, G. Portyankina, P. S. Russell, *Icarus* **205**, 296 (2010).
29. G. Portyankina, W. J. Markiewicz, N. Thomas, C. J. Hansen, M. Milazzo, *Icarus* **205**, 311 (2010).
30. S. Silvestro *et al.*, *Second International Dunes Conference, LPI Contributions*, **1552**, 65 (2010).
31. M. Mellon *et al.*, *J. Geophys. Res.* **114**, E00E07 (2009).
32. N. Putzig *et al.*, *Proc. Lunar Planet. Sci. Conf.* **41**, 1533 (2010).
33. R. Hayward *et al.*, *J. Geophys. Res.* **112** (E11), E11007 (2007).
34. K. Matsuo, K. Heki, *Icarus* **202**, 90 (2009).
35. L_s is the true anomaly of Mars in its orbit around the sun, measured from the martian vernal equinox, used as a measure of the season on Mars. $L_s = 0$ corresponds to the beginning of northern spring; $L_s = 180$ is the beginning of southern spring.

36. This work was partially supported by the Jet Propulsion Laboratory, California Institute of Technology, under a contract with NASA.

Supporting Online Material

www.sciencemag.org/cgi/content/full/331/6017/575/DC1
SOM Text
Fig. S1
References

10 September 2010; accepted 10 January 2011
10.1126/science.1197636

2500 Years of European Climate Variability and Human Susceptibility

Ulf Büntgen,[1,2]* Willy Tegel,[3] Kurt Nicolussi,[4] Michael McCormick,[5] David Frank,[1,2] Valerie Trouet,[1,6] Jed O. Kaplan,[7] Franz Herzig,[8] Karl-Uwe Heussner,[9] Heinz Wanner,[2] Jürg Luterbacher,[10] Jan Esper[11]

Climate variations influenced the agricultural productivity, health risk, and conflict level of preindustrial societies. Discrimination between environmental and anthropogenic impacts on past civilizations, however, remains difficult because of the paucity of high-resolution paleoclimatic evidence. We present tree ring–based reconstructions of central European summer precipitation and temperature variability over the past 2500 years. Recent warming is unprecedented, but modern hydroclimatic variations may have at times been exceeded in magnitude and duration. Wet and warm summers occurred during periods of Roman and medieval prosperity. Increased climate variability from ~250 to 600 C.E. coincided with the demise of the western Roman Empire and the turmoil of the Migration Period. Such historical data may provide a basis for counteracting the recent political and fiscal reluctance to mitigate projected climate change.

Continuing global warming and its potential associated threats to ecosystems and human health present a substantial challenge to modern civilizations that already experience many direct and indirect impacts of anthropogenic climate change (*1*–*4*). The rise and fall of past civilizations have been associated with environmental change, mainly due to effects on water supply and agricultural productivity (*5*–*9*), human health (*10*), and civil conflict (*11*). Although many lines of evidence now point to climate forcing as one agent of distinct episodes of societal crisis, linking environmental variability to human history is still limited by the dearth of high-resolution paleoclimatic data for periods earlier than 1000 years ago (*12*).

Archaeologists have developed oak (*Quercus* spp.) ring width chronologies from central Europe that cover nearly the entire Holocene and have used them for the purpose of dating archaeological artifacts, historical buildings, antique artwork, and furniture (*13*). The number of samples contributing to these records fluctuates between hundreds

[1]Swiss Federal Research Institute for Forest, Snow and Landscape Research (WSL), 8903 Birmensdorf, Switzerland. [2]Oeschger Centre for Climate Change Research, University of Bern, 3012 Bern, Switzerland. [3]Institute for Forest Growth, University of Freiburg, 79085 Freiburg, Germany. [4]Institute of Geography, University of Innsbruck, 6020 Innsbruck, Austria. [5]Department of History, Harvard University, Cambridge, MA 02138, USA. [6]Laboratory of Tree-Ring Research, University of Arizona, Tucson, AZ 85721, USA. [7]Environmental Engineering Institute, École Polytechnique Fédérale de Lausanne, 1015 Lausanne, Switzerland. [8]Bavarian State Department for Cultural Heritage, 86672 Thierhaupten, Germany. [9]German Archaeological Institute, 14195 Berlin, Germany. [10]Department of Geography, Justus Liebig University, 35390 Giessen, Germany. [11]Department of Geography, Johannes Gutenberg University, 55128 Mainz, Germany.

*To whom correspondence should be addressed. E-mail: buentgen@wsl.ch